Jpn. J. Cancer Res. **91**, 1285–1295, December 2000

In vivo and *in vitro* Interactions between Human Colon Carcinoma Cells and Hepatic Stellate Cells

Sadatoshi Shimizu,[1] Nobuya Yamada,[1,4] Tetsuji Sawada,[1] Kazuo Ikeda,[2] Norifumi Kawada,[3] Syuichi Seki,[3] Kenji Kaneda[2] and Kosei Hirakawa[1]

[1]Department of Surgery, [2]Department of Anatomy and [3]Department of Internal Medicine, Osaka City University Medical School, 1-4-3 Asahimachi, Abeno-ku, Osaka 545-8585

Stromal reaction is important for the growth of cancer both in primary and metastatic sites. To demonstrate this reaction during the hepatic metastasis of human colon carcinoma, we histologically investigated alterations to the distribution and phenotype of hepatic stellate cells (HSCs), the only mesenchymal cells in the liver parenchyma, using a nude mouse model. Intrasplenically injected colon carcinoma LM-H3 cells migrated into the space of Disse and underwent proliferation, in close association with hepatocytes and HSCs, at 2 days. At 14 days, HSCs were accumulated around the tumor mass and expressed α-smooth muscle actin, a marker for HSC activation. We next investigated *in vitro* the growth factors involved in the interactions between LM-H3 cells and HSCs. Conditioned medium of rat HSCs which underwent culture-induced activation contained platelet-derived growth factor (PDGF)-AB, hepatocyte growth factor (HGF) and transforming growth factor (TGF)-β, and could augment LM-H3-cell proliferation and migration. Neutralizing antibodies against PDGF-AA and PDGF-BB and those against PDGF-BB and HGF inhibited proliferation and migration, respectively, of LM-H3 cells, whereas antibody against TGF-β had no effect. LM-H3 cells expressed PDGF receptors-α and -β and c-met. Conditioned medium of LM-H3 cells contained PDGF-AB, and could enhance HSC proliferation and migration. This augmenting effect was suppressed by treatment with anti-PDGF-AB antibody. The present study has demonstrated that bidirectional interactions involving PDGF and HGF take place *in vitro* between colon carcinoma cells and HSCs, raising the possibility that similar interactions might be involved in the stromal reaction during hepatic metastasis.

Key words: Platelet-derived growth factor — Hepatocyte growth factor — Hepatic metastasis — Hepatic stellate cell — Colon carcinoma

In human colon carcinoma, hepatic metastasis implies a poor prognosis. This event involves several steps, i.e., exfoliation of cancer cells from the primary site, entry into the portal venous system, adhesion to the endothelium and subsequent extravasation in the hepatic microvasculature, and multiplication and formation of glandular or acinar structure in the liver parenchyma. Whether or not colon cancer cells successfully metastasize to the liver depends not only on their cytological properties, such as the cell-coat composition, but also on the hepatic microenvironment involving macrophages[1)] and natural killer cells,[2,3)] which constitute the defense system of the liver, and hepatic mesenchymal cells, which may support the growth of cancer cells.

In general, metastasized tumor cells modify the supporting mesenchymal tissue in which they grow. This phenomenon, termed stromal reaction, includes activation of fibroblasts or myofibroblastic transformation,[4,5)] enhanced secretion of matrix proteins[6,7)] and neovascularization,[8)] all of which promote proliferation and invasion of cancer cells.[9)] Myofibroblasts are usually associated with cancers of epithelial origin and contribute to the growth of metastatic tumors before neovascularization is induced.[10)] Stromal reaction takes place in colorectal carcinoma both in primary and metastatic sites; for example, stromal fibroblasts express activation markers such as α-smooth muscle actin (αSMA)[11)] and F19-antigen (or fibroblast activating protein-α)[12)] in association with tumor progression, and tumor-associated myofibroblasts enhance tumor invasiveness.[13)]

In the liver, hepatic stellate cells (HSCs) are the only mesenchymal cells present in the extravascular space of the liver parenchyma. While quiescent in the steady state, they are activated by various stimuli and undergo transformation into myofibroblasts, which are characterized by expression of αSMA,[14)] acquisition of contractility,[15)] enhanced secretion of growth factors such as transforming growth factor-β (TGF-β),[16)] platelet-derived growth factor (PDGF)[17,18)] and hepatocyte growth factor (HGF),[19)] and an increased production of extracellular matrix materials.[20,21)] Activated HSCs or transformed myofibroblasts

[4] To whom correspondence should be addressed.
E-mail: n-yamada@med.osaka-cu.ac.jp

also express receptors for PDGF-β[22] and TGF-β.[23] Recent *in vitro* studies have demonstrated that hepatic myofibroblasts promote the proliferation of hepatocellular carcinoma (HCC) cell lines, and the latter cells in turn activate and promote proliferation of the former cells.[24, 25] Similarly, hepatic metastasis of murine melanoma cells induces activation and proliferation of HSCs *in vivo* and induces them to release matrix metalloproteinase-2 and an unknown tumor-chemotactic factor, suggesting that tumor-induced HSC activation may contribute to the progression of hepatic metastasis.[26] There have been, however, no *in vivo* or *in vitro* studies on the interaction between HSCs and colon carcinoma cells.

We previously established a human colon carcinoma cell line LM-H3 which acquired a high metastatic capacity due to increased sialyl Lewis A expression and fucosyltransferase activity, and we developed a nude mouse model in which hepatic metastasis of human colon carcinoma can be experimentally analyzed.[27] In this study, to reveal the bidirectional interactions between human colon carcinoma cells and HSCs, we firstly demonstrated accumulation and activation of HSCs around hepatic metastasis of human colon carcinoma cells, and then investigated in the culture the growth factors involved in the enhanced proliferation and migration of activated HSCs and colon carcinoma cells.

MATERIALS AND METHODS

Animals Female BALB/c nude mice (4 weeks, Charles River Inc., Atsugi) and male Wistar rats (10–12 weeks, SLC, Shizuoka) were used for *in vivo* and *in vitro* studies, respectively. They were housed in specific-pathogen-free conditions and fed standard chow pellets and water *ad libitum*. Experiments were performed according to the standard guideline for animal experiments of the Osaka City University Medical School.

Tumor cells We used a highly metastatic colon carcinoma cell line LM-H3 obtained after three *in vivo* passages of a human colon cancer cell line OCUC-LM1, which was established from the liver metastasis of moderately differentiated adenocarcinoma of the colon in our laboratory.[27] LM-H3 cells were seeded in 10-cm culture dishes (Falcon, Lincoln Park, NJ) and cultured in 10 ml of Dulbecco's modified Eagle's medium (DMEM; Bioproducts, Walkersville, MD) containing 10% fetal bovine serum (FBS; Gibco, Grand Island, NY), 100 IU/ml penicillin (ICN Biomedicals, Costa Mesa, CA), 100 μg/ml streptomycin (ICN Biomedicals) and 0.5 m*M* sodium pyruvate (Bioproducts) at 37°C for 5 days until they became semi-confluent on the culture dish.

Formation of hepatic metastasis BALB/c nude mice were used. Under ether anesthesia, the abdomen was opened, and 1×10^7 cells/ml LM-H3 cells suspended in 0.1 ml of phosphate-buffered saline (PBS) were injected into the lower pole of the spleen. Splenectomy was conducted at 2–3 min after injection.

Histology At 1, 2, 3, 4 and 14 days after tumor cell injection, animals were sacrificed. Three mice were used at each time point. Under ether anesthesia, the liver was perfused via the portal vein first with PBS and then with either 1.5% glutaraldehyde in 0.067 *M* cacodylate buffer, pH 7.4, plus 1% sucrose or 4% paraformaldehyde in PBS.

Glutaraldehyde- or paraformaldehyde-fixed materials were post-fixed in 1% OsO_4 in 0.1 *M* phosphate buffer, pH 7.4, for 2 h, dehydrated in an ethanol series and embedded in Polybed (Polyscience Inc., Warrington, PA). Semithin sections were stained with toluidine blue and observed light-microscopically. Thin sections were stained with uranyl acetate and lead citrate and observed under a JEM1200EX electron microscope (JEOL, Tokyo) at 100 kV.

Paraformaldehyde-fixed materials were also embedded in OCT compound (Sakura Fine Technical Co., Tokyo) and frozen with liquid nitrogen. Cryosections were cut by a CM3050 cryostat (Leica Instruments GmbH, Nussloch, Germany). After incubation with normal animal serum for 30 min at room temperature, sections were incubated with primary antibodies overnight at 4°C. Primary antibodies used here were rabbit anti-desmin antibody (1:50, Monosan, Uden, Netherlands) and mouse anti-human αSMA monoclonal antibody (1A4, 1:500, DAKO, Carpenteria, CA). The sections were washed with PBS, and treated with 0.3% hydrogen peroxide in methanol to block endogenous peroxidase activity. They were then incubated with biotinylated swine anti-rabbit IgG antibody (1:500, DAKO) or anti-mouse IgG antibody (1:500, DAKO) for 30 min at room temperature, followed by incubation with avidin-biotin peroxidase complex (Vector Laboratories Inc., Peterborough, UK) for 60 min at room temperature. Immunoreactions were visualized by treating sections with 0.2 mg/ml 3,3′-diaminobenzidine tetrahydrochloride (DAB) in 0.05 *M* Tris-buffered saline, pH 7.4, in the presence of 0.003% hydrogen peroxide for 3–5 min. Counterstaining for nuclei was done with hematoxylin.

Isolation and culture of HSCs HSCs were isolated from the rat liver as previously reported.[15] Rats (300–400 g b.w.) were anesthetized with intraperitoneal injection of 0.1–0.2 ml/100 g b.w. pentobarbital. After canulation into the portal vein, the liver was perfused with SC-1 balanced salt solution [8 g/liter NaCl, 0.4 g/liter KCl, 88.17 mg/liter NaH_2PO_4-$2H_2O$, 120.45 mg/liter Na_2HPO_4, 2.38 g/liter HEPES, 0.19 g/liter EGTA, 0.9 g/liter glucose] at a flow rate of 10 ml/min for 10 min and subsequently with SC-2 solution [8 g/liter NaCl, 0.4 g/liter KCl, 88.17 mg/liter NaH_2PO_4-$2H_2O$, 120.45 mg/liter Na_2HPO_4, 2.38 g/liter HEPES, 0.35 g/liter $NaHCO_3$, 0.56 g/liter $CaCl_2$] containing 0.1% pronase E (Merck, Darmstadt, Germany)

for 10 min and then SC-2 solution containing 0.05% collagenase (Wako Pure Chemical Co., Osaka) for 25 min. The liver was excised and cut into small pieces, which were incubated in a shaking bath with SC-2 solution containing 0.05% pronase, 0.05% collagenase and 0.001% deoxyribonuclease (Boehringer, Mannheim, Germany) for 30 min at 37°C. Cells that passed through a 75-μm mesh were washed twice in Gey's balanced salt solution (GBSS/B; 8 g/liter NaCl, 0.37 g/liter KCl, 0.07 g/liter $MgSO_4$-$7H_2O$, 0.21 g/liter $MgCl_2$-$6H_2O$, 0.15 g/liter Na_2HPO_4-$12H_2O$, 0.03 g/liter KH_2PO_4, 1.09 g/liter glucose-H_2O, 0.227 g/liter $NaHCO_3$, 0.225 g/liter $CaCl_2$-$2H_2O$, 0.07 g/liter penicillin, 0.1 g/liter streptomycin) by centrifugation at 400*g* for 10 min. HSCs were purified by density gradient centrifugation with 8.2% Nycodenz (Nycomed Pharma AS, Oslo, Norway) at 1400*g* for 15 min at 4°C. A stellate cell-enriched fraction was obtained from an upper whitish layer. Cells were washed by centrifugation at 400*g* at 4°C for 10 min.

For culture, HSCs were suspended in DMEM supplemented with 10% FBS (Gibco) and antibiotics (0.035 g/liter penicillin and 100 mg/liter streptomycin) at the cell density of 5×10^5 cells/ml and cultured in 60-mm plastic dishes (Falcon). They were identified by the typical star-like configuration and vitamin A fluorescence. The purity was always higher than 95%, and the viability was more than 90% as evaluated by a trypan blue exclusion test. Because HSCs are activated at later than 3 days after culture, as represented by PDGFR-β expression,[28] we used 7-day cultured HSCs as activated HSCs for proliferation and migration assays.

Preparation of conditioned medium of cell culture At 6 h after seeding freshly isolated HSCs (5×10^5 cells/ml) in DMEM supplemented with 10% FBS, the medium was changed with 2 ml of serum-free DMEM. Serum-free conditioned medium of quiescent HSCs (qHSC-CM) was obtained by subsequent 2-day culture at 37°C. There was no significant decrease in cell viability of HSCs at 2 days compared to that of HSCs cultured with serum-containing DMEM. For the preparation of serum-free conditioned medium of activated HSCs (aHSC-CM), freshly isolated HSCs (5×10^5 cells/ml) were cultured in DMEM supplemented with 10% FBS for 2 days. After washing twice with DMEM, 2 ml of fresh serum-free DMEM was supplied. After a subsequent 5-day culture, aHSC-CM was obtained. Serum-free conditioned medium of cultured LM-H3 cells (LM-H3-CM) was prepared by incubating LM-H3 cells with serum-free DMEM at 37°C for 4 days.

Proliferation assay LM-H3 cells (2×10^5 cells/400 μl) or activated HSCs (2.5×10^5 cells/500 μl) were seeded into 24-well microplates (Falcon) and cultured with 400 μl of serum-free aHSC-CM or 500 μl of serum-free LM-H3-CM, respectively, for 3 days. Culture with serum-free DMEM was used as the control. Cells were harvested by 10-min trypsin digestion. Cell numbers were counted by a Coulter counter (Coulter Electronics, Luton, UK).

Migration assay Transwell double chambers with an 8-μm pore size (Costar, Cambridge, MA) were used. In the upper chamber were seeded LM-H3 cells (5×10^4 cells/100 μl) or activated HSCs (5×10^4 cells/100 μl), while the lower chamber contained 600 μl of serum-free aHSC-CM or 600 μl of serum-free LM-H3-CM, respectively. After 6-h culture at 37°C, cells remaining on the upper surface of filter were completely wiped away with a cotton swab, and the filter was stained with hematoxylin. The number of cells that had migrated to the lower surface of the filter was counted light-microscopically.

ELISA analysis of growth factors Growth factors involved in serum-free LM-H3-CM were quantitated by using ELISA kits for human PDGF-AB (Genzyme, Minneapolis, MN), human HGF (Genzyme), human TGF-β (R&D, Mineapolis, MN), human basic fibroblast growth factor (b-FGF; R&D), human epidermal growth factor (EGF; R&D), human interleukin-1-α (IL-1α; Genzyme), human IL-1β (Genzyme) and human tumor necrosis factor-α (TNF-α; R&D), and those in serum-free qHSC-CM and aHSC-CM were quantitated by using ELISA kits for human PDGF-AB (Genzyme) [human PDGF-AB has 95% homology with rat PDGF-AB; because an ELISA kit for PDGF-AA was not commercially available, we used a kit for PDGF-AB], rat HGF (Institute of Immunology, Tokyo), rat TGF-β (Morinaga, Kanagawa), human b-FGF (Genzyme) [human b-FGF has 95.5% homology with rat b-FGF] and rat TNF-α (Genzyme).

Treatments of cell culture with neutralizing antibodies In *in vitro* proliferation and migration assays for LM-H3 cells, rabbit anti-human PDGF-AA antibody (final concentration of 4, 40, 200 μg/ml; Genzyme), goat anti-human PDGF-BB antibody (6, 60, 300 ng/ml; Genzyme), goat anti-human HGF antibody (2, 20, 100 μg/ml; Genzyme) and rabbit anti-human TGF-β (1, 10, 50 μg/ml; Genzyme), and goat IgG standard (Chemicon International Inc., Temecula, CA) were added to the LM-H3 cell culture or the lower chamber supplemented with serum-free aHSC-CM. As controls, goat IgG standard (Chemicon International Inc.) or rabbit IgG standard (Cedarlane, Ontario, Canada) was used. In *in vitro* proliferation and migration assays for activated HSCs, goat anti-rat PDGF-AB (2, 20, 200 μg/ml, Upstate Biotechnology) was added to the HSC culture or the lower chamber in which serum-free LM-H3-CM was supplemented. As a control, goat IgG standard (Chemicon International Inc.) was used. Percent inhibition (%) was calculated as follows. Percent inhibition=(cell number in serum-free aHSC-CM or LM-H3-CM−cell number in serum-free aHSC-CM or LM-H3-CM treated with neutralizing antibodies or IgG standard)/(cell number in serum-free aHSC-CM or LM-H3-CM−cell number with serum-free DMEM alone)×100.

Flow cytometry To demonstrate the expression of PDGFR-α, PDGFR-β and c-met in LM-H3 cells, flow cytometric analysis was performed. A single cell suspension of LM-H3 cells was prepared by treatment with trypsin (Gibco). The cells were washed twice with cold FACS buffer [PBS with 0.01% sodium azide and 0.1% bovine serum albumin (BSA; Wako Pure Chemical Induscries, Ltd.)], and adjusted to 1×10^6 cells/200 μl. Subsequently, 2 μg of rabbit anti-PDGFR-α polyclonal antibody (Santa Cruz Biotechnology, Inc., Santa Cruz, CA), rabbit anti-PDGFR-β polyclonal antibody (Santa Cruz Biotechnology, Inc.) or rabbit anti-c-met polyclonal antibody (Santa Cruz Biotechnology, Inc.) was added to the cell suspension and the mixture was incubated for 30 min on ice. The cells were wahed with cold FACS buffer, then further incubated with 2 μg/200 μl of FITC-conjugated anti-rabbit IgG (Santa Cruz Biotechnology, Inc.) for 30 min on ice and analyzed with a Cell Quest (FACS Calibur, Becton Dickinson, San Jose, CA).

Statistics Data were expressed as the mean±standard deviation (SD). The significance of differences was analyzed by using the unpaired Student's *t* test.

RESULTS

Histological analysis of spatial association of LM-H3 cells with HSCs during the development of hepatic metastasis At one day after intrasplenic injection, LM-H3 cells were localized in the hepatic sinusoids, adhering to the endothelial cells (Fig. 1A). At 2 days, they migrated out of the sinusoids, entering the space of Disse (Figs. 1B, 2A) and making direct contact with HSCs (Fig. 2A, inset) and hepatocytes (Fig. 2A). At 3 days, they proliferated and formed micrometastatic foci preferentially in the periportal zone (Fig. 1C). Tumor cells were often arranged in a glandular structure, enclosing a lumen (Fig. 1C, 1D). They deeply invaded the hepatic cell plate and came into close apposition to the hepatocytes (Figs. 1D, 2B), with desmosomal junctions between them (Fig. 2B, inset). Due to expansion of the tumor mass, surrounding hepatocytes

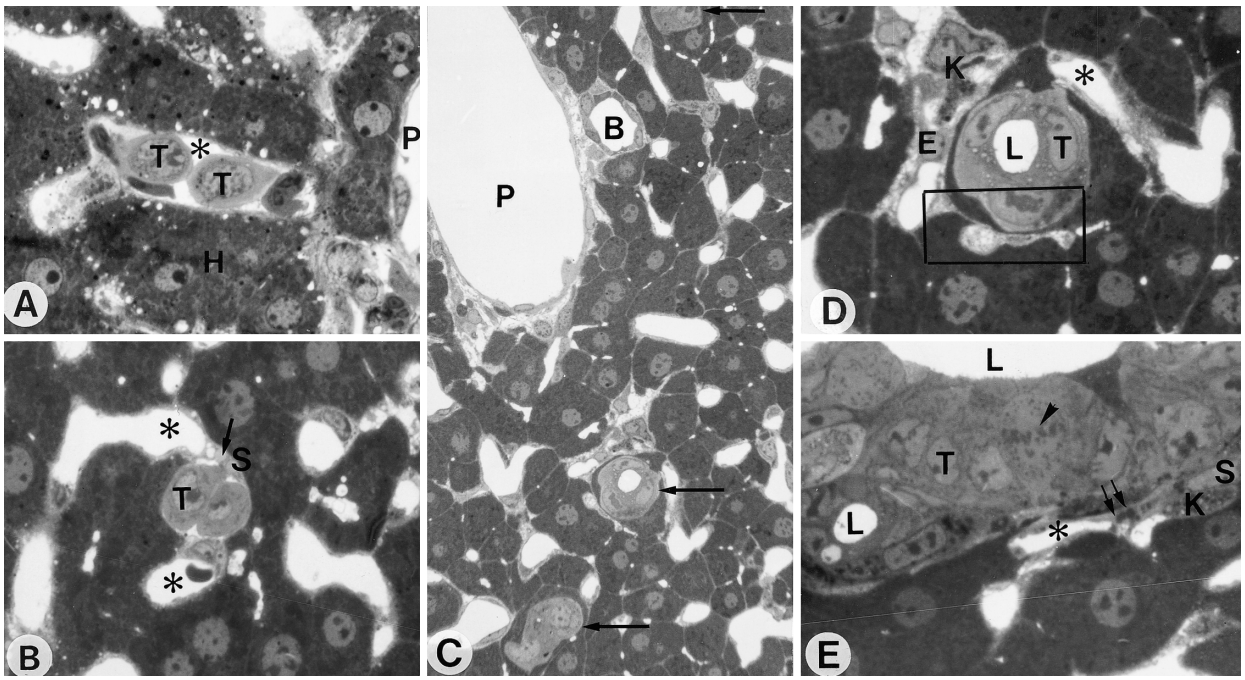

Fig. 1. Light micrographs of the hepatic metastasis of LM-H3 cells at 1 day (A), 2 days (B), 3 days (C, D) and 14 days (E) after intrasplenic injection. A. Tumor cells (T) are located within the sinusoidal lumen (asterisks) in the periportal zone. P, portal veins; H, hepatocytes. B. Tumor cells (T) are located outside the sinusoidal lumens (asterisks). HSCs (S) with lipid droplets (small arrow) are closely associated with tumor cells. C. A low-power micrograph shows the distribution of hepatic metastasis. Metastatic foci (large arrows) are preferentially distributed in the periportal zone. P, portal veins; B, bile ductules. D. Tumor cells (T) enclosing a lumen (L) are situated deeply in the hepatic cell plate, being surrounded by the attenuated cytoplasm of hepatocytes. K, Kupffer cells; E, endothelial cells; asterisks, sinusoidal lumen. E. Tumor cells (T) proliferate, showing a mitotic feature (arrowhead), and form a ductal structure with large and small lumens (L). Sinusoidal lumens (asterisks) are in close vicinity to the tumor masses. HSCs (S) with lipid droplets (small arrows) are situated in the periphery of tumor masses. K, Kupffer cells. A, B, D, E, ×700; C, ×320.

were considerably attenuated, and consequently, the distance between tumor cells and HSCs in adjacent sinusoids was greatly shortened (Fig. 2B). At 14 days, tumor masses enclosing a lumen increased in size in the space of Disse, facing the sinusoidal lumen in places (Fig. 1E). In such portions, HSCs made direct contact with tumor cells and

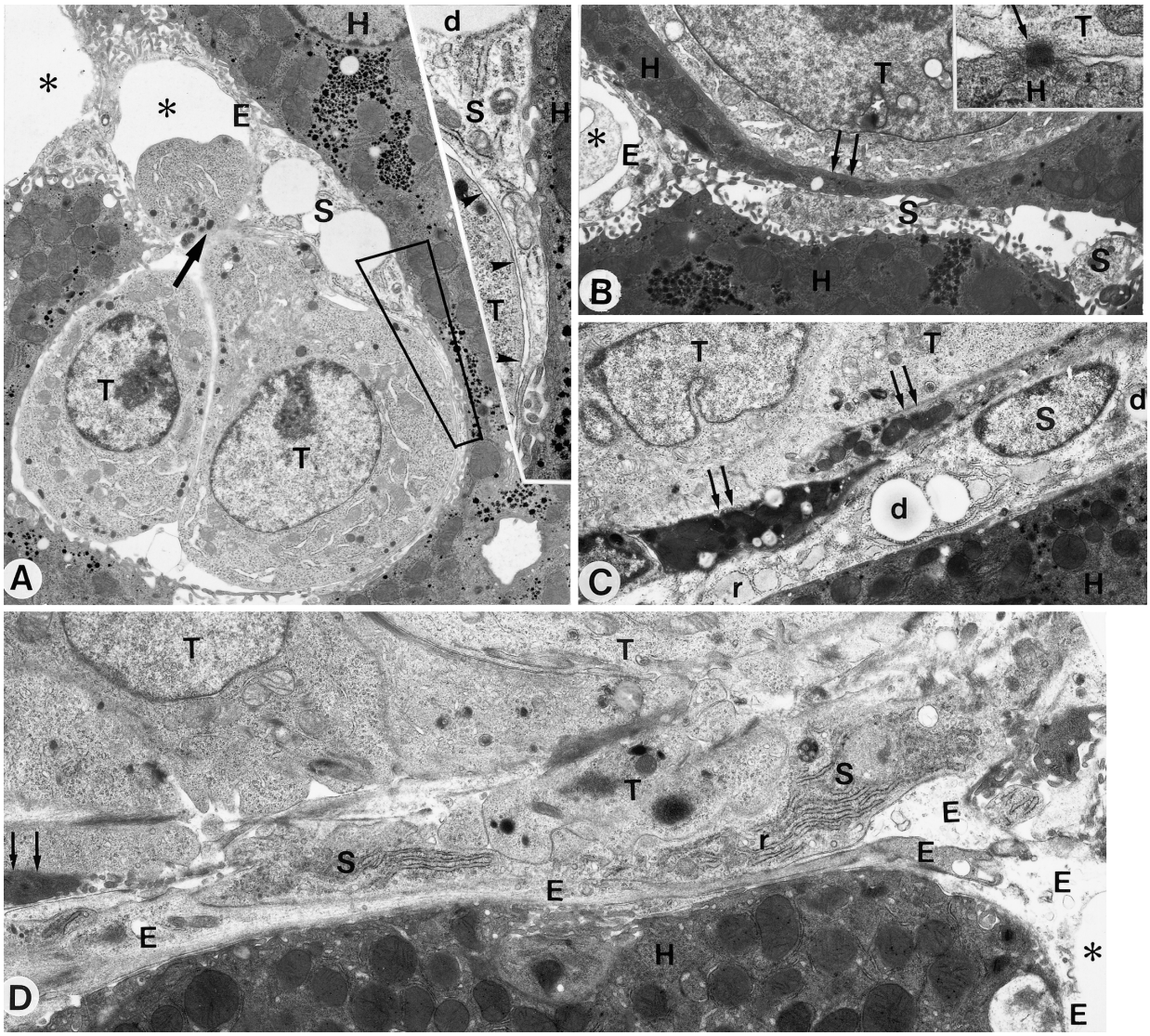

Fig. 2. Electron micrographs of the hepatic metastasis of LM-H3 cells at 2 days (A), 3 days (B) and 14 days (C, D) after intrasplenic injection. A. Electron microscopy of tumor cells (T) shown in Fig. 1B. They are situated in the space of Disse. An HSC (S) overlies a tumor cell, extending cytoplasmic processes along the cell surface, as indicated by arrowheads in the inset. A part of the cytoplasm of tumor cells protrudes from the pore (large arrow) of sinusoidal endothelial cells (E), suggesting extravasation at this site. H, hepatocytes; asterisks, sinusoidal lumen; d, lipid droplets. B. Electron microscopy of the rectangular portion of Fig. 1D. Tumor cells (T) invade the hepatocytes, making junctional specialization (arrow in inset) with hepatocytes (T). Due to expansion of tumor masses, surrounding hepatocytes are attenuated (double arrows), making the distance between tumor masses and HSCs (S) of adjacent sinusoids much shorter. E, endothelial cells. C & D. The boundary of the tumor depicted in Fig. 1E on hepatocytes. C. Fragments of hepatocellular cytoplasm (double arrows) are interposed between tumor cells (T) and HSCs (S), of which the latter contain lipid droplets (d) and dilated rough endoplasmic reticulum (r). The left one shows condensation of cytoplasm. D. In the portion facing the sinusoidal lumen (asterisks), HSCs (S) with well developed rough endoplasmic reticulum (r) are extended along the tumor mass, making a direct contact with tumor cells (T). There are endothelial cells (E) between HSCs and hepatocytes (H), suggesting sinusoidal obliteration here. A condensed, small cytoplasm of hepatocytes (double arrows) is seen. A, ×3800, inset, ×9500; B, ×4300, inset ×27 000; C, ×4500; D, ×7300.

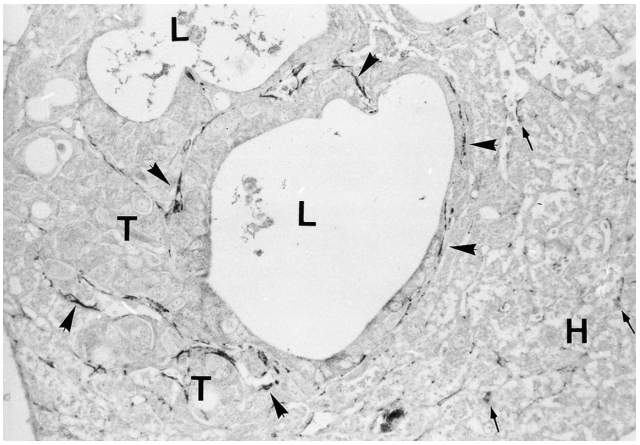

Fig. 3. Immunohistochemistry of the hepatic metastasis of LM-H3 cells for desmin at 14 days after intrasplenic injection. Desmin-positive cells are distributed in the normal liver parenchyma as indicated by arrows. They are accumulated around tumor cells (T), which exhibit a ductal structure with obvious lumens (L). H, hepatocytes. ×240.

further extended between tumor cells and hepatocytes together with endothelial cells, representing sinusoidal obliteration due to tumor expansion (Fig. 2D). Between tumor cells and HSCs were often found small parts of hepatocellular cytoplasm (Fig. 2C), probably derived from the attenuated cytoplasm shown in Fig. 2B.

Accumulation and activation of HSCs around the metastatic foci of LM-H3 cells When the tumor mass increased in size at 14 days, desmin-positive, spindle-shaped cells resembling HSCs were distributed more frequently around the metastatic foci than in the normal portion of liver parenchyma (Fig. 3). Until 4 days, αSMA was expressed exclusively in the perivascular smooth muscle cells of the portal vein and the central vein, and was not detected in the liver parenchyma, including the metastatic foci (Fig. 4, A and B). At 14 days, αSMA-positive cells were abundant around the metastatic foci (Fig. 4C). They were lined at the basal aspect of glandular structure, often facing the sinusoidal lumen (Fig. 4D).

***In vitro* proliferation and migration of LM-H3 cells was enhanced by serum-free aHSC-CM** To demonstrate the

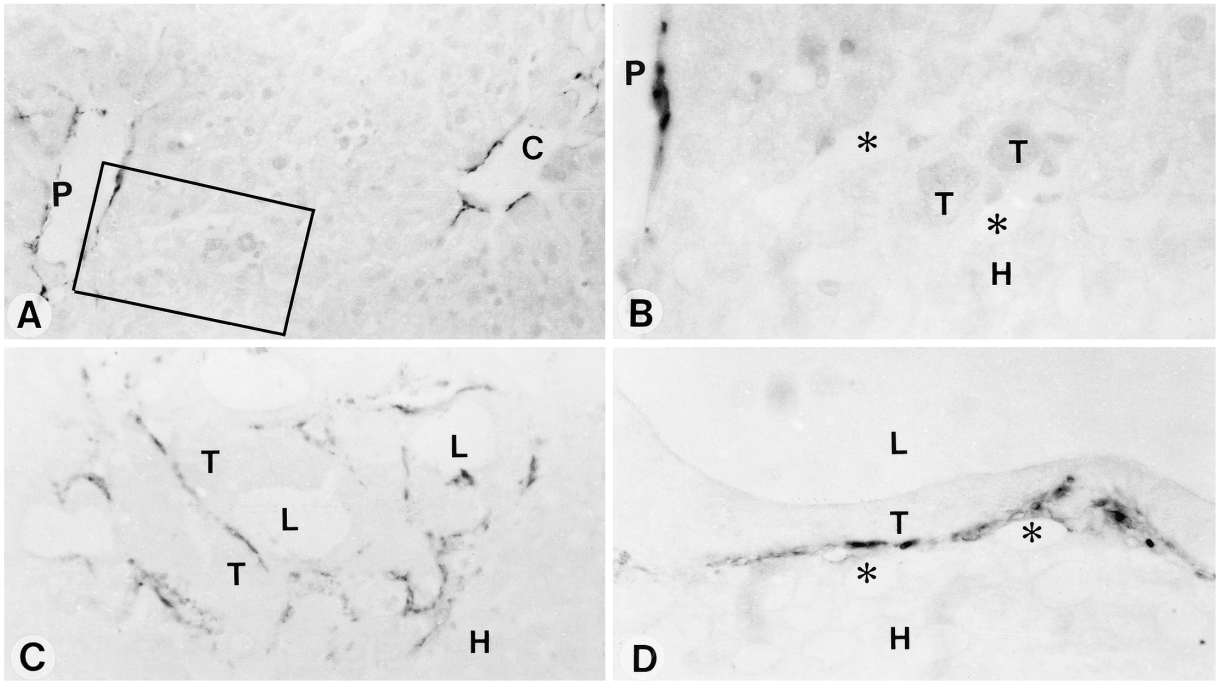

Fig. 4. Immunohistochemistry of the hepatic metastasis of LM-H3 cells for αSMA at 4 days (A, B) and 14 days (C, D) after intrasplenic injection. A. αSMA-positive cells are exclusively found around the portal veins (P) and central veins (C). B. Higher magnification of a rectangular portion of A. In the hepatic metastasis of tumor cells (T), no positive staining for αSMA is found. H, hepatocytes; asterisks, sinusoidal lumen. C. Around the tumor masses, αSMA-positive cells are abundant. They also invade the tumor masses. In the normal portion, no positive staining is found. H, hepatocytes. D. αSMA-positive cells are accumulated in the interface between tumor cells (T) and hepatocytes (H), often facing the sinusoidal lumens (asterisks). L, lumen of a ductular structure of tumor cells. A & C, ×240; B & D, ×600.

enhancing function of activated HSCs on proliferation and migration of LM-H3 cells, the effect of aHSC-CM on cultured LM-H3 cells was analyzed. In proliferation assay, serum-free aHSC-CM significantly increased the number of LM-H3 cells at 3 days compared to serum-free DMEM as a control (Fig. 5A). In migration assay, supplementation with serum-free aHSC-CM in the lower chamber induced migration of significantly larger numbers of LM-H3 cells at 6 h compared to that with serum-free DMEM (Fig. 5B).

***In vitro* proliferation and migration of activated HSCs was enhanced by serum-free LM-H3-CM** In proliferation assay, serum-free LM-H3-CM significantly increased the number of activated HSCs at 3 days compared to serum-free DMEM (Fig. 6A). In migration assay, introduction of serum-free LM-H3-CM into the lower chamber induced migration of significantly larger numbers of activated HSCs to the lower chamber at 6 h compared to that with serum-free DMEM (Fig. 6B).

Contents of growth factors and cytokines in serum-free LM-H3-CM, qHSC-CM and aHSC-CM The contents of growth factors and cytokines in serum-free LM-H3-CM, qHSC-CM and aHSC-CM were measured by ELISA analysis (Table I). Serum-free LM-H3-CM contained a large amount of PDGF-AB, but negligible amounts of HGF, TGF-β, EGF, b-FGF, IL-1α and TNF-α. Serum-free qHSC-CM contained HGF but not PDGF-AB or TGF-β, while serum-free aHSC-CM contained large amounts of PDGF-AB, HGF and TGF-β, but not b-FGF, IL-1α or TNF-α.

Suppressive effects of anti-growth factor antibodies on *in vitro* proliferation and migration of LM-H3 cells Treatment with anti-PDGF-AA antibody or with anti-PDGF-BB antibody significantly suppressed aHSC-CM-induced *in vitro* proliferation of LM-H3 cells, while that with anti-HGF antibody did not (Table II). Furthermore, treatment with anti-PDGF-BB antibody or with anti-HGF antibody significantly inhibited aHSC-CM-induced *in vitro* migration of LM-H3 cells, while that with anti-PDGF-AA antibody or with anti-TGF-β antibody did not (Table II).

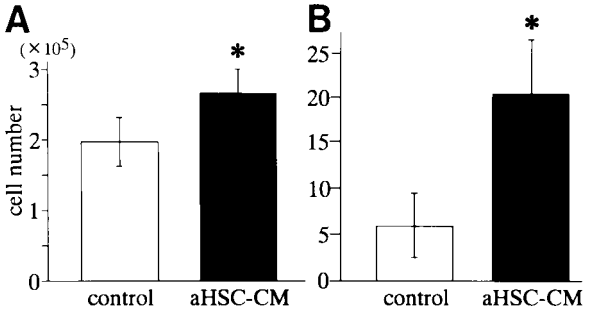

Fig. 5. Proliferation (A) and migration (B) of LM-H3 cells in serum-free DMEM and serum-free aHSC-CM. A. LM-H3 cells (2×10^5) were seeded in plastic dishes, and the cell numbers were counted at 3 days. Data represent the mean±SD (n=5). * P<0.01. B. LM-H3 cells (5×10^5) were seeded in the upper chamber, and the number of cells migrating into the lower chamber was counted at 6 h. Data represent the mean±SD (n=5). * P<0.01.

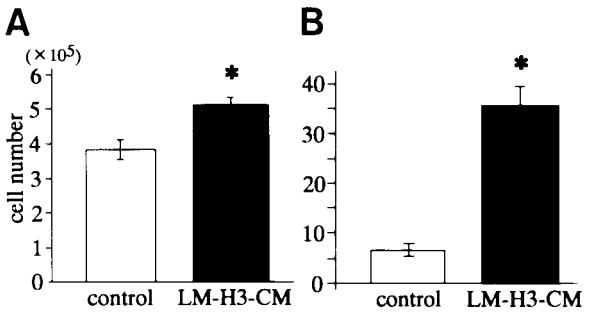

Fig. 6. Proliferation (A) and migration (B) of activated HSCs in serum-free DMEM and serum-free LM-H3-CM. A. Activated HSCs (2×10^5) were seeded on plastic dishes, and the cell numbers were counted at 3 days. Data represent the mean±SD (n=5). * P<0.01. B. Activated HSCs (5×10^5) were seeded in the upper chamber, and the number of cells migrating into the lower chamber was counted at 6 h. Data represent the mean±SD (n=5). * P<0.01.

Table I. Contents (pg/ml) of Growth Factors and Cytokines in Serum-free LM-H3-CM and HSC-CM (from Quiescent and Activated HSCs) as Determined by ELISA[a)]

Conditioned medium	PDGF-AB	HGF	TGF-β	EGF	b-FGF	IL-1α	TNF-α
LM-H3-CM	753	0	0	2.1	6.8	0	<5.0
HSC-CM							
quiescent HSCs	10	3200	0	n.t.[b)]	n.t.	n.t.	n.t.
activated HSCs	3000	5850	3633	n.t.	3.5	0	0

a) Data are representative of 6 independent experiments.
b) n.t., not tested.

Table II. Inhibition of Serum-free aHSC-CM-induced LM-H3 Cell Proliferation and Migration by Treatment with Neutralizing Antibodies against Growth Factors[a)]

Growth factor	Doses of IgG or Ab	Percent inhibition (%)			
		Proliferation		Migration	
		IgG[b)]	Neutralizing Abs	IgG	Neutralizing Abs
PDGF-AA	4 μg/ml	1.7±4.1	−0.8±1.5	3.5±1.4	1.8±3.1
	40 μg/ml	2.1±3.9	16.8±3.7*	9.0±3.8	3.5±2.4
	200 μg/ml	n.t.[c)]	n.t.	7.2±3.6	8.9±1.9
PDGF-BB	6 ng/ml	0.7±1.3	9.7±1.5*	−4.3±12.1	26.5±4.9*
	60 ng/ml	−2.7±1.6	12.3±1.5*	−4.1±7.9	33.2±6.0*
	300 ng/ml	n.t.	n.t.	−2.5±16.2	33.2±11.7*
HGF	2 μg/ml	−11.2±1.9	−0.3±2.9	−3.0±9.1	36.4±4.1*
	20 μg/ml	−20.0±4.4	−3.5±3.2	17.1±3.6	46.8±5.7*
	100 μg/ml	n.t.	n.t.	2.0±3.5	74.5±1.9*
TGF-β	1 μg/ml	n.t.	n.t.	3.2±5.8	−8.2±7.4
	10 μg/ml	n.t.	n.t.	3.0±10.1	3.1±7.3
	50 μg/ml	n.t.	n.t.	3.3±9.9	−3.2±21.6

a) Data are representative of 2–3 independent experiments. Data are expressed as the mean±SD (n=6 and 4 samples for proliferation assay and migration assay, respectively). * P<0.01 versus IgG control.
b) As the control for αPDGF-AA and αTGF-β , rabbit IgG was used, and as the control for αPDGF-BB and αHGF, goat IgG was used.
c) n.t., not tested.

Table III. Inhibition of Serum-free LM-H3-CM-induced HSC Proliferation and Migration by the Treatment with Neutralizing Antibody against PDGF[a)]

Growth factor	Dose of IgG or Ab (μg/ml)	Percent inhibition (%)			
		Proliferation		Migration	
		IgG[b)]	Neutralizing Ab	IgG	Neutralizing Ab
PDGF-AB[c)]	2	−0.6±5.2	20.9±5.9*	12.1±1.0	60.7±5.2*
	20	4.3±6.8	34.1±2.6*	−5.6±5.4	62.5±7.9*
	200	n.t.[d)]	n.t.	23.9±5.7	83.4±5.9*

a) Data are representative of 3 independent experiments. Data are expressed as the mean±SD (n=4 samples). * P<0.01 versus IgG control.
b) As the control for αPDGF-AB, goat IgG was used.
c) Anti-PDGF-AB antibody neutralizes all of PDGF-AA, PDGF-AB and PDGF-BB.
d) n.t., not tested.

Suppressive effects of anti-growth factor antibodies on *in vitro* proliferation and migration of activated HSCs Because only PDGF-AB was detected in LM-H3-CM among the growth factors and cytokines examined here (Table I), we investigated the suppressive effect of a neutralizing antibody against PDGF-AB (we used this antibody because a neutralizing antibody against rat PDGF-BB was not commercially available). Treatment with anti-PDGF-AB antibody significantly inhibited LM-H3-CM-induced *in vitro* proliferation and migration of activated HSCs (Table III).

Expression of PDGFR-α, PDGFR-β and c-met in LM-H3 cells To reveal the expression of PDGFR-α, PDGFR-β and c-met in LM-H3 cells, flow cytometric analysis was conducted. The proportions of positive cells for PDGFR-α, PDGFR-β and c-met were 56.2%, 54.9% and 59.5%, respectively (Fig. 7).

DISCUSSION

The present study using a nude mouse model[27] demonstrated that human colon carcinoma cells which metasta-

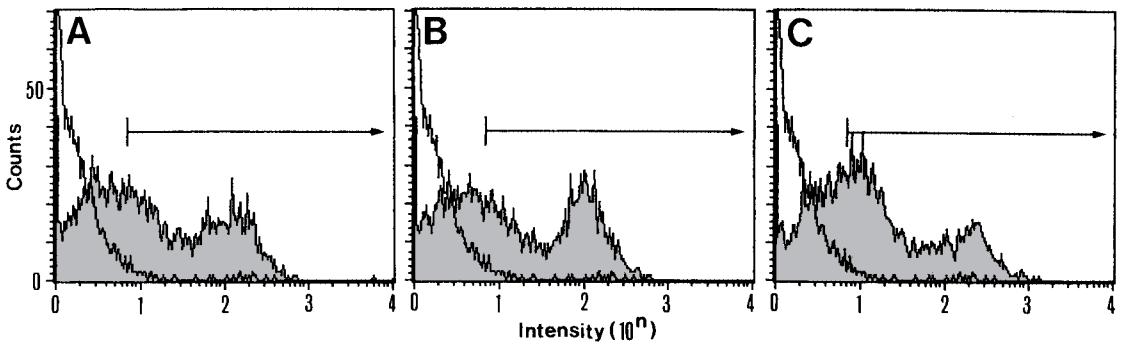

Fig. 7. Flow cytometric analysis of PDGFR-α (A), PDGFR-β (B) and c-met (C) expression in LM-H3 cells (shaded portion). The proportions of PDGFR-α, PDGFR-β and c-met positive cells with staining intensity larger than 7×10^0 (indicated by arrows) are 51.5%, 50.5% and 53.7%, respectively.

size to the liver associated closely with HSCs. Unlike murine melanoma cells, which are often used for experiments on hepatic metastasis, LM-H3 cells deeply invaded the hepatic cell plate and multiplied there, being surrounded by hepatocytes, but not in the space of Disse. They were arranged in a glandular structure in the liver parenchyma, making desmosomal junctions with apposed hepatocytes. Although the functional significance of such a tumor growth pattern is not known, Yamori *et al.*[29] demonstrated using murine and human colon carcinoma cell lines that a hepatocyte-derived growth factor different from PDGF and FGF had a tumor-growth-promoting activity, suggesting its role in the regulation of selective survival and colonization in the liver. In addition to the close apposition to the hepatocytes, LM-H3 cells retained direct contact with HSCs which surrounded the sinusoid from which tumor masses received their blood supply. As the tumor increased in size, the cytoplasm of the hepatocytes enclosing tumor cells was considerably attenuated and ultimately torn off, thus making nearby HSCs join the peritumoral accumulation of HSCs.

Immunohistochemical study demonstrated that peritumoral HSCs were more frequent than HSCs in the surrounding normal parenchyma, suggesting their local proliferation or migration. Furthermore, while quiescent at days 2–4, they became activated by day 14, as represented by positive staining for αSMA. These results indicate that, in spite of cytological and architectural differences from murine melanoma cells, LM-H3 cells induced similar peritumoral accumulation and activation of HSCs.

Because close association and probable interaction between LM-H3 cells and HSCs were suggested by the present *in vivo* study, we next investigated the growth factors involved in the interactions between them *in vitro*. The appropriateness of this *in vitro* model using human tumor cells and rat HSCs is supported by the high homology of amino acid sequences of PDGF-AA, PDGF-BB, HGF and TGF-β between humans and rats, i.e., 95.7%, 89.0%, 91.6% and 99.1%, resepectively, according to the manufacturers' documentation. Serum-free aHSC-CM, which contained PDGF-AB, HGF and TGF-β, significantly augmented proliferation and migration of LM-H3 cells, and this proliferation was inhibited by neutralizing antibodies against PDGF-AA and PDGF-BB, while migration was inhibited by antibodies against PDGF-BB and HGF, consistent with previous data that binding of PDGF-AA or PDGF-BB with PDGFR-α preferentially induces proliferation, while that of PDGF-BB with PDGFR-β leads to proliferation and migration.[30] These data suggest that PDGF-AA and/or BB and HGF secreted by activated HSCs play important roles in inducing LM-H3 cell proliferation and migration. Responsiveness of LM-H3 cells to these growth factors was supported by their expression of PDGFR-α PDGFR-β and c-met. The present results are also consistent with the previous findings that PDGF-BB promoted the growth of colon cancer cells *in vivo*,[31] and HGF increased the invasiveness of two HCC cell lines (HepG2 and HuH7) *in vitro*.[24] In the latter experiment, however, HGF showed opposite effects on proliferation in the two cell lines, and, furthermore, PDGF had no appreciable effect on them,[24] suggesting that responsiveness to growth factors may vary among tumor cell lines or types. In contrast to PDGF and HGF, TGF-β, which inhibits tumor growth early in progression,[32] had no effect on LM-H3 cell migration.

Action of LM-H3 cells directed to activated HSCs was also demonstrated *in vitro*. Serum-free LM-H3-CM containing PDGF-AB but not HGF and TGF-β induced proliferation and migration of activated HSCs. It is reported that activated HSCs express PDGFR-α and PDGFR-β and undergo proliferation and migration in response to PDGF-AA and PDGF-BB.[18, 28, 33–35] Taking this into account, the present results suggest that PDGF may be responsible for augmenting the effects of LM-H3-cells on activated HSCs.

Nakamura *et al.*[36] reported that PDGF and interleukin (IL)-1 derived from tumor cells played a role in inducing HGF expression in stromal cells, which in turn led to the invasive growth of carcinoma cells. Because activated HSCs also produce PDGF-AB, which could act on them in an autocrine manner, the functional significance of the paracrine action of LM-H3-cell-derived PDGF-AB on activated HSCs needs to be further investigated.

The mechanism of HSC activation by tumor cells is not well understood. Olaso *et al.* supposed that quiescent HSC-activating factors might be released from metastatic melanoma cells.[26] Some human and rat colon cancer cell lines are reported to produce TGF-β,[37, 38] which stimulates HSCs to transform into myofibroblast-like cells and enhances their production of extracellular matrix proteins.[20, 39, 40] In this study, LM-H3 cells did not secrete TGF-β, but secreted PDGF-AB instead. An inducing function of PDGF in HSC activation has been reported.[41] Rat HCC cell lines which induced HSC activation, on the other hand, failed to produce PDGF-BB.[25] Therefore, different kinds of growth factors might be involved in HSC activation in different tumors.

In conclusion, there are mutual interactions involving PDGF and HGF between cultured colon carcinoma cells and HSCs, suggesting that similar interactions may be present in the hepatic metastasis of human colon carcinoma.

(Received June 17, 2000/Revised August 18, 2000/Accepted August 26, 2000)

REFERENCES

1) Williams, D. L., Sherwood, E. T., McNamee, R. B., Jones, E. L. and Di-Luzio, N. R. Therapeutic efficacy of glucan in a murine model of hepatic metastatic disease. *Hepatology*, **5**, 198–206 (1985).
2) Kaneda, K. and Wake, K. Ultrastructural study of *in vivo* tumor lysis by liver-associated natural killer cells. *Biomed. Res.*, **11**, 137–143 (1990).
3) Shiratori, Y., Nakata, R., Okano, K., Komatsu, Y., Shiina, S., Kawase, T., Sugimoto, T., Omata, M. and Tanaka, M. Inhibition of hepatic metastasis of colon carcinoma by asialo-GM1-positive cells in the liver. *Hepatology*, **16**, 469–478 (1992).
4) Tsukamoto, H., Mishima, Y., Hayashibe, K. and Sasase, A. Alpha-smooth muscle actin expression in tumor and stromal cells of benign and malignant human pigment cell tumors. *J. Invest. Dermatol.*, **98**, 116–120 (1992).
5) Rønnov-Fenssen, L., Petersen, O. W., Koteliansky, V. E. and Bissel, M. J. The origin of the myofibroblasts in breast cancer: recapitulation of tumor environment in culture unravels diversity and implicates converted fibroblasts and recruited smooth muscle cells. *J. Clin. Invest.*, **95**, 859–873 (1995).
6) Knudson, W., Biswas, C. and Toole, B. P. Interactions between human tumor cells and fibroblast stimulate hyaluronate synthesis. *Proc. Natl. Acad. Sci. USA*, **81**, 6767–6771 (1985).
7) Merrilees, M. and Finlay, G. Human tumor cells in culture stimulate glycosaminoglycan synthesis by human skin fibroblasts. *Lab. Invest.*, **53**, 30–36 (1985).
8) Tanaka, H., Konno, H., Matsuda, I., Nakamura, S. and Baba, S. Prevention of hepatic metastasis of human colon carcinoma by angiogenesis inhibitor TNP-470. *Cancer Res.*, **55**, 836–839 (1995).
9) Grégoire, M. and Lieubeau, B. The role of fibroblasts in tumor behaviour. *Cancer Metastasis Rev.*, **14**, 339–350 (1995).
10) Schmitt-Gräff, A., Desmoulière, A. and Babbiani, G. Heterogeneity of myofibroblast phenotypic features an example of fibroblastic cell plasticity. *Virchows Arch.*, **425**, 3–24 (1994).
11) Lieubeau, B., Garrigue, L., Barbieux, I., Meflah, K. and Grégoire, M. The role of transforming growth factor β1 in the fibroblastic reaction associated with rat colorectal tumor development. *Cancer Res.*, **54**, 6526–6532 (1994).
12) Welt, S., Divgi, C. R., Scott, A. M., Garin-Chesa, P., Finn, R. D., Graham, M., Carswell, E. A., Cohen, A., Larson, S. M., Old, L. J. and Rettig, W. J. Antibody targeting in metastatic colon cancer: a phase I study of monoclonal antibody F19 against a cell-surface protein of reactive tumor stromal fibroblasts. *J. Clin. Oncol.*, **12**, 1193–1203 (1994).
13) Dimanche-Boitrel, M. T., Vakaet, L., Pujuguet, P., Chauffert, B., Martin, M. S., Hammann, A., Van Roy, F., Mareel, M. and Martin, F. *In vivo* and *in vitro* invasiveness of a rat colon-cancer cell line maintaining E-cadherin expression: an enhancing role of tumor-associated myofibroblasts. *Int. J. Cancer*, **56**, 512–521 (1994).
14) Ramadori, G., Veit, T. and Schwogler, S. Expression of the gene of the alpha-smooth muscle-actin isoform in rat liver and in rat fat-storing (Ito) cells. *Virchows Arch. B Cell Pathol.*, **59**, 349–357 (1990).
15) Kawada, N., Tran-Thi, T. A., Klein, H. and Decker, K. The contraction of hepatic stellate (Ito) cells stimulated with vasoactive substances. Possible involvement of endothelin-1 and nitric oxide in the regulation of the sinusoidal tonus. *Eur. J. Biochem.*, **213**, 815–823 (1993).
16) Bachem, M. G., Meyer, D., Melchior, R., Sell, K. M. and Gressner, A. M. Activation of rat liver lipocytes by transforming growth factors derived from myofibroblast like cells. A potential mechanism of self perpetuation in liver fibrogenesis. *J. Clin. Invest.*, **89**, 19–27 (1992).
17) Win, K. M., Charlotte, F., Mallat, A., Cherqui, D., Martin, N., Mavier, P., Preaux, A. M., Dhumeaux, D. and Rosenbaum, J. Mitogenic effect of transforming growth factor-β1 on human Ito cells in culture: evidence for mediation by endogenous platelet-derived growth factor. *Hepa-*

tology, **18**, 137–145 (1993).
18) Marra, F., Choudhury, G. G., Pinzani, M. and Abboud, H. E. Regulation of platelet-derived growth factor secretion and gene expression in human liver fat-storing cells. *Gastroenterology*, **107**, 1110–1117 (1994).
19) Skrtic, S., Wallennius, V., Ekberg, S., Brenzel, A., Gressner, A. M. and Jansson, J. O. Hepatocyte-stimulated expression of hepatocyte growth factor (HGF) in cultured rat hepatic stellate cell. *J. Hepatol.*, **30**, 115–124 (1999).
20) Friedman, S. L. The cellular basis of hepatic fibrosis. *N. Engl. J. Med.*, **25**, 1828–1835 (1993).
21) Casini, A., Pinzani, M., Milani, S., Grappone, C., Galli, G., Jezequel, A. M., Schuppan, D., Rotella, C. M. and Surrenti, C. Regulation of extracellular matrix synthesis by transforming growth factor β1 in human fat-storing cells. *Gastroenterology*, **105**, 245–253 (1993).
22) Wong, L., Yamasaki, G., Johnson, R. J. and Friedman, S. L. Induction of β-PDGFR in rat hepatic lipocytes during cellular activation *in vivo* and in culture. *J. Clin. Invest.*, **94**, 1563–1569 (1995).
23) Lalazar, A., Wong, L., Yamasaki, G. and Friedman, S. L. Early genes induced in hepatic stellate cells during wound healing. *Gene*, **195**, 235–243 (1997).
24) Neaud, V., Faouzi, S., Guirouilh, J., Bail, B. L., Balabaud, C., Bioulac-Sage, P. and Rosenbaum, J. Human hepatic myofibroblasts increase invasiveness of hepatocellular carcinoma cells: evidence for a role of hepatocyte growth factor. *Hepatology*, **26**, 1458–1466 (1997).
25) Faouzi, S., Lepreux, S., Bedin, C., Dubuisson, L., Balabaud, C., Bioulac-Sage, P., Desmoulière, A. and Rosenbaum, J. Activation of cultured rat hepatic stellate cells by tumoral hepatocytes. *Lab. Invest.*, **79**, 485–493 (1999).
26) Olaso, E., Santisteban, A., Bidaurranzaga, J., Gressner, A. M., Rosenbaum, J. and Vidal-Vanaclocha, F. Tumor-dependent activation of rodent hepatic stellate cells during experimental melanoma metastasis. *Hepatology*, **26**, 634–642 (1997).
27) Yamada, N., Chung, Y.-S., Takatsuka, S., Arimoto, Y., Sawada, T., Dohi, T. and Sowa, M. Increased sialyl Lewis A expression and fucosyltransferase activity with acquisition of a high metastatic capacity in a colon cancer cell line. *Br. J. Cancer*, **76**, 582–587 (1997).
28) Ikeda, K., Wakahara, T., Wang, Y.-Q., Kadoya, H., Kawada, N. and Kaneda, K. *In vitro* migratory potential of rat quiescent hepatic stellate cells and its augmentation by cell activation. *Hepatology*, **29**, 1760–1767 (1999).
29) Yamori, T., Shimada, K., Kanda, H., Nishizuru, Y., Komi, A., Yamazaki, K., Asanoma, K., Ogawa, M., Nomura, K., Nemoto, N., Kumada, K. and Tsuruo, T. Establishment of a hepatocyte cell line producing growth-promoting factors for liver-colonizing tumor cells. *Jpn. J. Cancer Res.*, **87**, 146–152 (1996).
30) Claesson-Welsh, L. Platelet-derived growth factor receptor signals. *J. Biol. Chem.*, **51**, 32023–32026 (1994).
31) Hsu, S., Huang, F. and Friedman, E. Platelet-derived growth factor-B increases colon cancer cell growth *in vivo* by a paracrine effect. *J. Cell. Physiol.*, **165**, 239–245 (1995).
32) Hsu, S., Huang, F., Winawer, S. and Friedman, E. Colon carcinoma cells switch their response to TGFβ1 with tumor progression. *Cell Growth Diff.*, **5**, 267–275 (1994).
33) Marra, F., Gentilini, A., Pinzani, M., Choudhury, G. G., Parola, M., Herbst, H., Dianzani, M. U., Laffi, G., Abboud, H. E. and Gentilini, P. Phosphatidylinositol 3-kinase is required for platelet-derived growth factor's actions on hepatic stellate cells. *Gastroenterology*, **112**, 1297–1306 (1997).
34) Friedman, S. L. and Arthur, M. J. P. Activation of cultured rat hepatic lipocytes by Kupffer cell conditioned medium. Direct enhancement of matrix synthesis and stimulation of cell proliferation via induction of platelet-derived growth factor receptors. *J. Clin. Invest.*, **84**, 1780–1785 (1989).
35) Pinzani, M., Gesualdo, L., Sabbah, G. M. and Abboud, H. E. Effects of platelet-derived growth factor and other polypeptide mitogens on DNA synthesis and growth of cultured rat liver fat-storing cells. *J. Clin. Invest.*, **84**, 1786–1793 (1989).
36) Nakamura, T., Matsumoto, K., Kiritoshi, A., Tano, Y. and Nakamura, T. Induction of hepatocyte growth factor in fibroblasts by tumor-derived factors affects invasive growth of tumor cells: *in vitro* analysis of tumor-stromal interactions. *Cancer Res.*, **57**, 3305–3313 (1997).
37) Coffey, R. J., Shipley, G. D. and Moses, H. L. Production of transforming growth factors by human colon cancer lines. *Cancer Res.*, **46**, 1164–1169 (1986).
38) Grégoire, M., Garrigue, L., Blottière, H. M., Denis, M. G. and Meflah, K. Possible involvement of TGFβ1 in the distinct tumorigenic properties of two rat colon carcinoma clones. *Invasion Metastasis*, **12**, 185–196 (1992).
39) Matsuoka, M. and Tsukamoto, H. Stimulation of hepatic lipocyte collagen production by Kupffer cell-derived transforming growth factor beta: implication for a pathogenetic role in alcoholic liver fibrogenesis. *Hepatology*, **11**, 599–605 (1990).
40) Gressner, A. M. and Bachem, M. G. Molecular mechanisms of liver fibrosis—a homage to the role of activated fat-storing cells. *Digestion*, **56**, 335–346 (1995).
41) Gressner, A. M. Cytokines and cellular crosstalk involved in the activation of fat-storing cells. *J. Hepatol.*, **22**, 28–36 (1995).